

Recoil Properties of Rare-Earth Nuclides Produced by the Interaction of 28-GeV Protons with Uranium and Gold*

J. B. Cumming and K. Bächmann†

Chemistry Department, Brookhaven National Laboratory, Upton, New York 11973

(Received 7 June 1972)

The thick-target-thick-catcher technique was used to determine the recoil properties of some rare-earth nuclides produced by the interaction of 28-GeV protons with uranium and gold. Mean momenta derived from this and other experiments are discussed in terms of fission and spallationlike processes. It is concluded that, while fission can account for neutron-rich products from uranium, the momenta of neutron-deficient rare-earth nuclides from both uranium and gold are too low to arise from any conventional fission process. In the mass region below the rare earths, many neutron-deficient isotopes appear to be formed by mixed mechanisms. Only the most neutron-deficient products have momenta as low as those predicted for a spallationlike process. Mean cascade deposition energies, E^* , derived from the forward to backward ratios average 145 MeV for the neutron-deficient rare earths from uranium and 199 MeV for these products from gold. Such low values for gold and the even lower values for uranium cannot be understood in terms of a model for the spallationlike process involving a nucleonic cascade followed by conventional evaporation. Either there is a breakdown of the two-step model, e.g. as might be expected if fragment emission is involved, or it is not valid to extrapolate to 28 GeV the momentum-transfer excitation-energy relationship inferred from Monte Carlo calculations at much lower energies.

INTRODUCTION

There is now a rather large body of experimental data which indicates that at least two mechanisms contribute to forming products in the mass region just below the rare earths from uranium targets irradiated with multi-GeV protons. From cross section measurements¹⁻⁹ it can be inferred that charge dispersion curves in the vicinity of mass 131 are double peaked. Results at 28 GeV as summarized by Chu *et al.*¹⁰ show a broad peak (which may have some fine structure) on the neutron-rich side of β stability, a shallow valley at $Z_A - Z \approx -1$,¹¹ and a neutron-deficient peak centered at $Z_A - Z \approx -2.5$.

Studies^{1, 2, 9, 12-15} of recoil properties of products in this region indicate that neutron-rich species have mean ranges and kinetic energies typical of those expected for fission fragments, while neutron-deficient products have kinetic energies smaller by a factor of 2 to 3. Recent measurements by Beg and Porile⁹ indicate that the neutron-deficient products ¹²⁸Ba and ¹³¹Ba have fissionlike ranges for bombarding energies up to ≈ 1 GeV, and that the decrease in mean range takes place between ≈ 1 and ≈ 6 GeV, with only slight variation at higher energies. Forward to backward (F/B) ratios for these products reach a maximum value at ≈ 3 GeV and then decrease between 3 and 11.5 GeV. Such results undoubtedly indicate changes in mechanism in the 1-6-GeV region. Quantitative analy-

sis by Beg and Porile showed that neither fission nor spallation in a conventional sense could account for the ¹²⁸Ba and ¹³¹Ba results at 11.5 GeV. By including processes involving the emission of fragments such as ²⁴Na in an approximate manner, they were able to account for many of the observed properties.

Momentum spectra of barium isotopes formed from uranium by 2.2-GeV protons^{13, 15} indicate rather smooth trends as a function of neutron richness of the product. It was concluded that fission of nuclei near uranium could account for ¹⁴⁰Ba production, but that lower-mass fissioning species (extending down to approximately bismuth) were necessary to explain lower most-probable momenta observed for ¹²⁸Ba and ¹³¹Ba. In addition, low-momentum components [< 50 (MeV amu)^{1/2}] were seen in the spectrum of ¹³¹Ba and to a still greater extent in that of ¹²⁸Ba. These were considered as arising from a spallationlike process, but it could not be determined whether fragments were associated with their production.

Solid-state detector measurements¹⁶ have confirmed that there is a rather wide range of fissioning species involved in uranium fission induced by 2.9-GeV protons. For collinear fragments, contributions from asymmetric-mode fission of nuclei near uranium with high kinetic energy release could be seen. For fragment pairs deviating from collinearity, symmetric-mode fission with lower kinetic energy release was ob-

served indicating lower-mass fissioning species. However, no momenta as low as the low-momentum components of the radiochemically determined spectra^{13, 15} were seen, and it was concluded that they must arise from some process distinctly different from binary fission.

The aim of the present experiment was to extend recoil measurements into the rare-earth region for products of the interaction of 28-GeV protons with uranium. Cross section measurements^{10, 17} in this region have indicated that the neutron-rich and neutron-deficient peaks of the charge dispersion curve are more clearly separated at mass ≈ 147 than they are at mass ≈ 131 . It was anticipated that interpretation of recoil data in terms of mechanisms would be simpler with the reduced overlap between peaks. For comparison purposes some recoil studies of rare-earth products from gold targets were also performed to examine a situation where the contribution from fission is much reduced.

EXPERIMENTAL RESULTS AND ANALYSIS

Data presented in this paper are obtained from the same set of experiments which had been used for the measurements of cross sections¹⁷ and the experimental procedures have been outlined in that paper. In brief summary, a target consisting of a heavy metal foil (≈ 68 mg/cm² in the case of uranium or 104 mg/cm² for gold), covered on the upstream and downstream sides by stacks of three ≈ 7 -mg/cm² aluminum foils, was irradiated

TABLE I. Recoil properties of rare-earth nuclides produced by the interaction of 28-GeV protons with uranium.

Nuclide	Type	$2w(F+B)$ (mg/cm ²)	$w(F-B)$ (mg/cm ²)	F/B
¹³⁴ Ce	C	2.35 ± 0.08	0.23 ± 0.04	1.50 ± 0.11
¹³⁹ Ce	P	2.32 ± 0.04	0.15 ± 0.02	1.29 ± 0.05
¹³⁹ Nd	C	2.49 ± 0.13	0.17 ± 0.06	1.31 ± 0.14
¹⁴⁰ Nd	C	2.61 ± 0.12	0.22 ± 0.06	1.39 ± 0.13
¹⁴⁵ Eu	C	2.00 ± 0.08	0.14 ± 0.04	1.31 ± 0.10
¹⁴⁶ Eu	I	2.81 ± 0.07	0.19 ± 0.03	1.30 ± 0.07
¹⁴⁶ Gd	C	1.62 ± 0.12 ^a	0.14 ± 0.02	1.42 ± 0.09
¹⁴⁷ Eu	I	2.70 ± 0.10	0.16 ± 0.05	1.28 ± 0.10
¹⁴⁷ Gd	C	2.45 ± 0.08 ^a	0.26 ± 0.04	1.55 ± 0.09
¹⁴⁹ Gd	P	2.24 ± 0.10 ^a	0.24 ± 0.03	1.54 ± 0.08
¹⁴¹ Ce	C	7.18 ± 0.21 ^a	0.32 ± 0.12 ^a	1.19 ± 0.08 ^a
¹⁴³ Ce	C	7.63 ± 0.23	0.26 ± 0.12	1.15 ± 0.07
¹⁴⁴ Ce	C	7.86 ± 0.31 ^a	0.19 ± 0.12	1.10 ± 0.07
¹⁴⁷ Nd	C	6.12 ± 0.19	0.16 ± 0.10	1.10 ± 0.07
¹⁵³ Sm	C	6.85 ± 0.36	0.12 ± 0.18	1.07 ± 0.11
¹⁵⁶ Sm	C	7.59 ± 0.42	0.07 ± 0.21	1.02 ± 0.12

^a Errors have been increased to reflect disagreement between duplicate experiments.

with 28-GeV protons in the Brookhaven alternating gradient synchrotron. Prior to irradiation the leading edges of all seven foils were carefully aligned. The proton beam entered the foils perpendicular to the large dimensions of the stack. After irradiation the heavy metal foil and the adjacent aluminum catchers on the upstream and downstream sides were removed and separately processed radiochemically to give samples of individual rare-earth elements. Specific nuclides were assayed in these samples by β , positron, x-ray, or γ -ray measurements. Duplicate determinations were performed with uranium and gold targets, although some of the shorter-lived isotopes were not measured in the second experiment with gold.

Three quantities are of significance in an experiment such as this: F , the fraction of the total activity (target plus catchers) of a particular nuclide found in the forward recoil catcher; B , the corresponding fraction found in the backward catcher; and w , the thickness of heavy metal foil in mg/cm². Following common practice,¹⁸ we present in Tables I and II values of $2w(F+B)$, $w(F-B)$, and F/B instead of the directly measured quantities, as these derived quantities are more convenient for subsequent discussion and analysis. The values of $2w(F+B)$ and $w(F-B)$ have been corrected for preferential scattering into the aluminum at the heavy-metal catcher interface. This correction was based on the comparisons by Niday¹⁹ of $2w(F+B)$ values obtained using lead catchers with those using aluminum catchers for products of the thermal fission of uranium. Values listed in Tables I and II are weighted means in those cases where duplicate determinations were performed. The weight of an individual determination was tak-

TABLE II. Recoil properties of rare-earth nuclides produced by the interaction of 28-GeV protons with gold.

Nuclide	Type	$2w(F+B)$ (mg/cm ²)	$w(F-B)$ (mg/cm ²)	F/B
¹³⁴ Ce	C	1.87 ± 0.18 ^a	0.31 ± 0.04	2.00 ± 0.20
¹³⁹ Nd ^b	C	1.60 ± 0.11	0.27 ± 0.06	2.00 ± 0.28
¹⁴⁰ Nd	C	1.48 ± 0.07 ^a	0.25 ± 0.03	2.02 ± 0.17
¹⁴⁵ Eu	C	1.38 ± 0.03	0.26 ± 0.01	2.22 ± 0.11
¹⁴⁶ Eu	I	1.27 ± 0.10 ^a	0.22 ± 0.03 ^a	2.08 ± 0.11
¹⁴⁶ Gd	C	1.31 ± 0.09 ^a	0.24 ± 0.03	2.16 ± 0.11
¹⁴⁷ Eu	I	1.33 ± 0.07 ^a	0.26 ± 0.02	2.28 ± 0.19
¹⁴⁷ Gd	C	1.45 ± 0.09 ^a	0.33 ± 0.02	2.70 ± 0.12
¹⁴⁹ Gd	P	1.11 ± 0.05 ^a	0.22 ± 0.02	2.35 ± 0.17
¹⁵¹ Tb ^b	C	1.30 ± 0.07	0.27 ± 0.04	2.39 ± 0.28
¹⁵² Tb ^b	C	1.39 ± 0.20	0.27 ± 0.10	2.25 ± 0.71
¹⁵³ Tb ^b	C	1.26 ± 0.21	0.31 ± 0.10	2.93 ± 0.97
¹⁵⁵ Dy ^b	C	1.00 ± 0.12	0.20 ± 0.06	2.36 ± 0.62

^a Errors have been increased to reflect disagreement between duplicate experiments.

^b Results from a single experiment.

en to be the reciprocal of the variance of the value as calculated from external error estimates including uncertainties from counting statistics, analysis of the γ spectra, and/or resolution of decay curves. Internal errors were also calculated from the agreement of the duplicate determinations. In 57 of the 72 duplicates determined, the standard error of the mean obtained from the agreement of duplicates was smaller than that obtained from external error estimates. However, for 15 of the entries in the tables agreement was poorer than expected. The errors reported in Tables I and II have been taken to be the larger of the two possible values. It should be noted that the cases of disagreement are heavily concentrated in the columns giving $2w(F+B)$. The reason for this effect is now known, but it is clear if agreement between duplicates had been used as the sole error criterion, most of the standard errors in Tables I and II would have been smaller. However, no systematic effects have been included.

The nuclides in Table I are divided into two classes. The first 10 isotopes are neutron-deficient products, the last six are neutron rich. For each nuclide, a type symbol is given. A C (cumulative yield) indicates that the β -decaying precursors of the product had decayed prior to chemical separation. An I (independent) indicates essentially no β -decay feeding of the product and a P (partial) shows an intermediate situation. In the case of the gold targets (Table II), only neutron-deficient products could be observed.

Some general features can be seen from Tables I and II without a more detailed analysis. The neutron-rich products have mean ranges [as approximated by $2w(F+B)$] about 3 times as large

as those of the neutron-deficient products, an even greater difference than was seen in the iodine¹² and antimony¹⁴ regions. The products from gold have smaller mean ranges than the neutron-deficient products from uranium. The F/B values show the reverse trend. Neutron-rich products from uranium are nearly isotropic (i.e., F/B is near unity). Neutron-deficient products from uranium are more forward peaked, and for gold the forward direction is favored by a factor of 2 or more.

To proceed further with the analysis of the data, assumptions must be made as to the mechanism of the nuclear reactions involved. In the conventional two-step model,¹⁸ the observed velocity of a recoil \vec{v}_i is resolved into components \vec{v} and \vec{V} due to the first (or cascade) and second (or deexcitation) steps of the reaction, respectively. The components of \vec{v} , parallel and perpendicular to the beam direction, are designated v_{\parallel} and v_{\perp} . The vector \vec{V} (magnitude V) is assumed to have an isotropic angular distribution. Furthermore, if the range R_i (in the heavy-element target material) of a recoil having a speed v_i can be approximated by

$$R_i = \text{const} \times v_i^N, \quad (1)$$

where N is a constant, the following approximations can be derived:

$$2w(F+B) = R \left[1 + \frac{(N+1)^2}{4} \eta_{\parallel}^2 \right] \quad (2)$$

and,

$$w(F-B) = \eta_{\parallel} R \left[\frac{N+2}{3} \right]. \quad (3)$$

In these equations, R is the mean range in the tar-

TABLE III. Recoil parameters of rare-earth nuclides produced by the interaction of 28-GeV protons with uranium.

Nuclide	R (mg/cm ²)	η_{\parallel}	$\langle Z \rangle$	T (MeV)	v_{\parallel} [(MeV/amu) ^{1/2}]
¹³⁴ Ce	2.32 ± 0.08	0.076 ± 0.014	58.5	15.6 ± 0.6	0.037 ± 0.007
¹³⁹ Ce	2.31 ± 0.04	0.047 ± 0.007	58.4	14.6 ± 0.3	0.022 ± 0.003
¹³⁹ Nd	2.47 ± 0.13	0.051 ± 0.020	60.5	16.4 ± 0.9	0.025 ± 0.010
¹⁴⁰ Nd	2.66 ± 0.12	0.062 ± 0.018	60.8	17.7 ± 0.9	0.031 ± 0.009
¹⁴⁵ Eu	1.98 ± 0.08	0.052 ± 0.015	63.6	13.1 ± 0.6	0.022 ± 0.006
¹⁴⁶ Eu	2.79 ± 0.07	0.050 ± 0.010	63.0	18.5 ± 0.6	0.025 ± 0.005
¹⁴⁶ Gd	1.60 ± 0.12	0.067 ± 0.012	64.4	10.7 ± 0.8	0.026 ± 0.005
¹⁴⁷ Eu	2.68 ± 0.10	0.046 ± 0.015	63.0	17.4 ± 0.7	0.022 ± 0.007
¹⁴⁷ Gd	2.42 ± 0.08	0.082 ± 0.011	64.7	16.2 ± 0.6	0.038 ± 0.005
¹⁴⁹ Gd	2.20 ± 0.10	0.083 ± 0.010	65.1	14.4 ± 0.7	0.037 ± 0.004
¹⁴¹ Ce	7.17 ± 0.20	0.040 ± 0.015	56.0	53.2 ± 2.1	0.035 ± 0.013
¹⁴³ Ce	7.62 ± 0.23	0.031 ± 0.014	56.6	57.6 ± 2.7	0.028 ± 0.013
¹⁴⁴ Ce	7.85 ± 0.31	0.022 ± 0.014	56.9	59.9 ± 3.7	0.020 ± 0.013
¹⁴⁷ Nd	6.12 ± 0.19	0.023 ± 0.015	58.1	41.5 ± 1.8	0.017 ± 0.011
¹⁵³ Sm	6.85 ± 0.36	0.016 ± 0.024	59.9	47.0 ± 3.5	0.013 ± 0.019
¹⁵⁸ Sm	7.59 ± 0.42	0.008 ± 0.044	60.6	53.3 ± 3.9	0.007 ± 0.036

get material corresponding to the recoil speed V and η_{\parallel} is defined as v_{\parallel}/V . It was assumed in the derivation of Eqs. (2) and (3) that v_{\perp} was zero. Examination of the more complete equations²⁰ which include η_{\perp} ($=v_{\perp}/V$) terms, indicates that only very small changes would result if $v_{\perp} \neq 0$. Somewhat larger effects (but still small) would result if the assumption of isotropy for V is not justified. Experimental angular distributions for products such as ^{131}Ba and ^{103}Pd from uranium¹³ and ^{149}Tb from gold²¹ are consistent with isotropy at a bombarding energy of 2.2 GeV. However, a significant anisotropy (15%) was observed¹³ for ^{140}Ba from uranium. From the more detailed equations which include such anisotropy we find R would be increased by 2.7% and η_{\parallel} would be decreased by 2.2% as compared to values from the simplified equations.

From the data of Tables I and II values of R and η_{\parallel} were obtained using Eqs. (2) and (3). For the low-range products from uranium and gold N was assumed to be 2.0. For the neutron-rich products from uranium N was taken as 1.34 following Sugarman *et al.*²² It should be noticed that R is nearly independent of the choice of N for the small values of η_{\parallel} observed in this work. On the other hand, η_{\parallel} is more sensitive to the choice of N . Values of R and η_{\parallel} are listed in columns 2 and 3 of Tables III and IV. Perhaps more meaningful are the mean kinetic energy, T , and v_{\parallel} derived from R and η_{\parallel} .

The range-velocity relationships used for this conversion will be described elsewhere.²³ They are based on the tables of path lengths given by Northcliffe and Schilling²⁴ with semiempirical corrections for path-length projected-range differences. In converting mean projected range R to kinetic energy, an average precursor charge, $\langle Z \rangle$, given in column 4 of Tables III and IV was used.

Values of $\langle Z \rangle$ were obtained from the published charge-dispersion curves for uranium,¹⁰ and assumed to be the same in the case of gold. It should be noted that range is nearly proportional to kinetic energy for the low-range fragments in uranium and gold; hence $\langle T \rangle$ can be directly obtained from R . On the other hand, for the neutron-rich products for uranium, the relationship $R = kV - \delta$ is more appropriate and a $\langle V \rangle$ is obtained from R . Since the velocity spectra of these neutron-rich species are probably quite narrow,¹³ not much error is introduced by the assumption that $\langle V^2 \rangle = \langle V \rangle^2$ in calculating T .

The velocity spectra of neutron-deficient products from both gold²¹ and uranium¹³ are broad. Furthermore correlations between v_{\parallel} and V have been inferred^{13,21}; hence the conversion of a value of $\eta_{\parallel} = \langle v_{\parallel}/V \rangle$ into a value of $\langle v_{\parallel} \rangle$ is not straightforward. The values listed in Tables III and IV are equal to $\eta_{\parallel} \langle V^2 \rangle^{1/2}$ which is about the best we can do with thick-target data. To estimate potential errors in such an evaluation of $\langle v_{\parallel} \rangle$, we can use the parameters $\langle 1/V \rangle$ and $\langle V^2 \rangle^{1/2}$ of the V distribution inferred from thin-target studies of ^{149}Tb production from gold at 2.2 GeV.²¹ In the absence of correlations

$$\frac{\langle v_{\parallel} \rangle_{\text{calc}}}{\langle v_{\parallel} \rangle_{\text{true}}} = \left\langle \frac{1}{V} \right\rangle \langle V^2 \rangle^{1/2} = 1.41;$$

hence, values of $\langle v_{\parallel} \rangle$ listed in the tables for the low-range products may be substantially overestimated.

DISCUSSION

Mean momenta of rare-earth isotopes produced by the interaction of 28-GeV protons with uranium are plotted as a function of neutron richness of the product in Fig. 1. Mean momenta are ob-

TABLE IV. Recoil parameters of rare-earth nuclides produced by the interaction of 28-GeV protons with gold.

Nuclide	R (mg/cm ²)	η_{\parallel}	$\langle Z \rangle$	T (MeV)	v_{\parallel} [(MeV/amu) ^{1/2}]
^{134}Ce	1.80 ± 0.18	0.13 ± 0.02	58.4	10.4 ± 1.1	0.052 ± 0.007
^{139}Nd	1.54 ± 0.11	0.13 ± 0.02	60.5	8.6 ± 0.6	0.046 ± 0.009
^{140}Nd	1.42 ± 0.07	0.13 ± 0.01	60.8	7.8 ± 0.4	0.044 ± 0.005
^{145}Eu	1.31 ± 0.03	0.15 ± 0.01	63.6	7.2 ± 0.2	0.047 ± 0.003
^{146}Eu	1.22 ± 0.10	0.14 ± 0.01	63.0	6.5 ± 0.5	0.041 ± 0.003
^{146}Gd	1.26 ± 0.08	0.14 ± 0.01	64.4	6.9 ± 0.4	0.044 ± 0.003
^{147}Eu	1.26 ± 0.07	0.16 ± 0.01	63.0	6.6 ± 0.4	0.046 ± 0.004
^{147}Gd	1.35 ± 0.08	0.19 ± 0.01	64.7	7.3 ± 0.4	0.058 ± 0.003
^{149}Gd	1.05 ± 0.05	0.16 ± 0.01	65.1	5.6 ± 0.3	0.043 ± 0.003
^{151}Tb	1.23 ± 0.07	0.16 ± 0.02	66.2	6.4 ± 0.4	0.047 ± 0.006
^{152}Tb	1.32 ± 0.19	0.15 ± 0.05	66.4	6.8 ± 1.0	0.045 ± 0.016
^{153}Tb	1.15 ± 0.19	0.20 ± 0.05	66.6	5.8 ± 0.9	0.055 ± 0.015
^{155}Dy	0.95 ± 0.11	0.16 ± 0.04	67.3	4.7 ± 0.5	0.039 ± 0.011

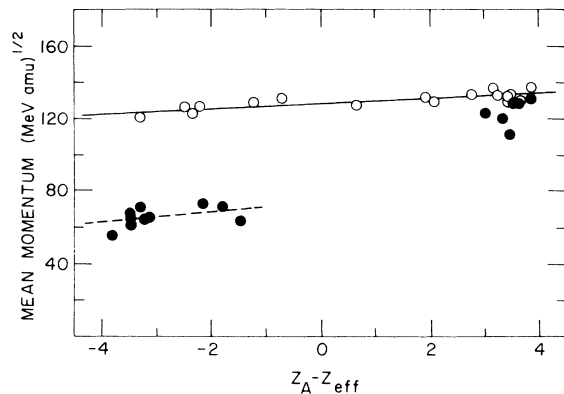


FIG. 1. Dependence of mean momentum of various rare-earth nuclides formed by the interaction of protons with uranium on the distance of the product from β stability. The abscissa $Z_A - Z_{\text{eff}}$ is discussed in the text. The filled points are from the present work at 28 GeV. The open circles are from the results of Hogan and Sugarman (Ref. 25) at 0.45 GeV.

tained from kinetic energies listed in Tables III and IV via the relationship, $P = \sqrt{2AT}$. Choice of $Z_A - Z_{\text{eff}}$ as the abscissa of this figure follows the suggestion of Chu *et al.*¹⁰ who observed that cross-section data formed a more consistent pattern when plotted vs $Z_A - Z_{\text{eff}}$ than when the neutron to proton ratio was used. Values of Z_A , the position of β stability at a given mass, were obtained from their work. Z_{eff} is in most cases the same as $\langle Z \rangle$ in Table III; however, small corrections have been made for shell effects using the procedure of Chu *et al.*¹⁰ where appropriate.

For comparison with the 28-GeV results, momenta of rare-earth products obtained at 0.45 GeV by Hogan and Sugarman²⁵ are also shown in Fig. 1. At the lower energy, product momenta on both sides of stability are high and the dependence on

$Z_A - Z_{\text{eff}}$ is slight. The solid least-squares line increases from 123 (MeV amu)^{1/2} at $Z_A - Z_{\text{eff}} = -3.5$ to 133 (MeV amu)^{1/2} at $+3.5$. Mean momenta of neutron-rich products at 28 GeV remain high, with the most neutron-rich species ¹⁴⁴Ce and ¹⁵⁶Sm falling close to the values at 0.45 GeV. By contrast, momenta of neutron-deficient products observed in the present work are about a factor of 2 lower than those observed at 0.45 GeV. The observations of Beg and Porile⁹ on ¹²⁸Ba and ¹³¹Ba suggest that this decrease occurs at bombarding energies between 1 and 6 GeV. The pattern shown in Fig. 1 is qualitatively the same as has been observed in the studies of antimony¹⁴ and iodine¹² isotopes at 0.59 and 18 GeV, but the magnitude of the decrease in momentum of the neutron-deficient products is larger.

In preparing Fig. 1 we have converted the mean ranges given by Hogan and Sugarman²⁵ into momenta using the same range-velocity assumptions which had been used for the 28-GeV data. They originally used rather different range-velocity curves which led to a steeper dependence on $Z_A - Z_{\text{eff}}$ [mean momenta of 112 (MeV amu)^{1/2} at $Z_A - Z_{\text{eff}} = -3.5$ and 128 (MeV amu)^{1/2} at $+3.5$]. It is interesting to note that the conclusions drawn by Hogan and Sugarman²⁵ concerning changes in the mean separation distance between charge centers in the fission process depend critically on the slope of this line, which, in turn appears to depend on the range-velocity assumption.

There is now available a substantial body of recoil data for products of the interaction of uranium with protons having energies above 10 GeV. It appears from the results of Beg and Porile⁹ that mean momenta will not depend strongly on bombarding energy above 10 GeV; hence we can compare the results of studies of antimony isotopes by Hagebø and Ravn¹⁴ at 19 GeV, those of Brandt¹²

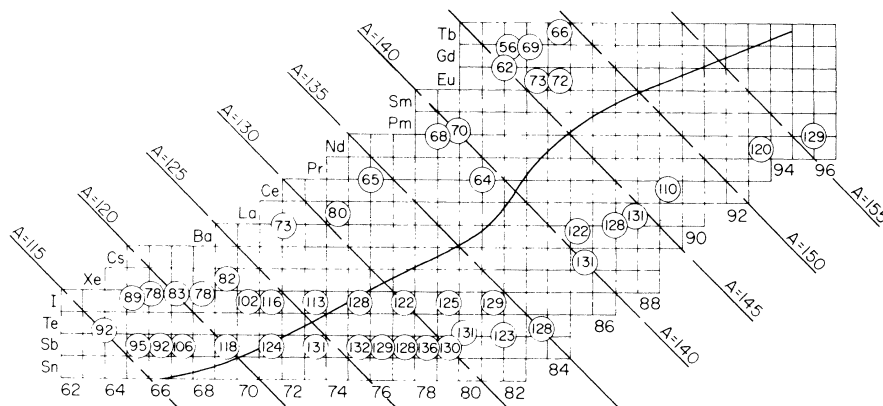


FIG. 2. Mean moments of products of the interaction of high-energy (>10 -GeV) protons with uranium as a function of neutron and proton number. The approximate position of the line of β stability is shown by the heavy line. Data are obtained from the present work and Refs. 9, 12, and 14.

on iodine at the same energy, the data on barium isotopes at 11.5 GeV obtained by Beg and Porile,⁹ and the rare-earth results obtained in the present experiment at 28 GeV. For this purpose we have converted published mean ranges to momenta using our range-velocity relationships. A general picture is given in Fig. 2 where mean momenta are shown in circles superimposed on a section of an isotope chart. The centers of the circles are located at N and Z coordinates which reflect β -decay feeding where appropriate. The heavy line traces the line of β stability in this mass region. It can be seen that products on the neutron-rich side of stability have high mean momenta [≥ 120 (MeV amu)^{1/2}] with the exception of the 110 (MeV amu)^{1/2} value observed for ¹⁴⁷Nd in the present work. The source of this anomalous value for ¹⁴⁷Nd is not known. To the left of β stability mean momenta decrease; however, except at the lower masses in this region, the position of the decrease is not well established. It is clear that more measurements near β stability in the rare-earth region would be desirable.

We will now proceed to examine the dependence of mean momentum, $\langle P \rangle$, on $Z_A - Z_{\text{eff}}$ and A in more detail and to make comparisons with the dependence of cross sections on the same variables. Mean momenta for products having masses between 115 and 135 are plotted as a function of $Z_A - Z_{\text{eff}}$ in Fig. 3. For comparison the charge-dispersion curve for $A = 131$ given by Chu *et al.*¹⁰ is also shown. Mean momenta of products in the broad neutron-rich peak are seen to be high and nearly independent of $Z_A - Z_{\text{eff}}$, consistent with

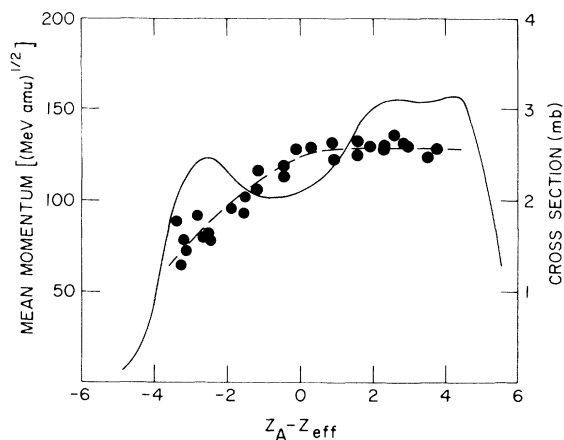


FIG. 3. Comparison between mean momenta of products of the interaction of high-energy protons (≥ 10 GeV) with uranium and the charge-dispersion curve. Mean momenta, shown by points, are for masses $115 \leq A \leq 135$ from Refs. 9, 12, 14, and the present work. The solid curve gives the charge dispersion reported by Chu *et al.* (Ref. 10) for $A = 131$.

fission as a formation mechanism. For $Z_A - Z_{\text{eff}} < 0$, momenta decrease in an approximately linear manner with increasing neutron deficiency. There does not appear to be a sharp drop in momenta at the position of the minimum in the charge-dispersion curve. We conclude that most of the neutron-deficient products in this region are formed by mixed mechanisms as we would not expect the momentum of a spallationlike product to be very sensitive to $Z_A - Z_{\text{eff}}$.

Figure 4 presents the analogous data for products of heavier mass. Recoil data for masses 139 to 156 have been shown together with the charge dispersion¹⁰ for $A = 147$. The paucity of data in the vicinity of stability precludes any strong statement on the dependence of $\langle P \rangle$ on $Z_A - Z_{\text{eff}}$. However, it does appear that variation in the vicinity of the neutron-deficient peak is less than seen at the lower masses. This may indicate a cleaner reaction mechanism in contrast to the apparently mixed situation at $A = 131$. The shape of the charge-dispersion curves tends to imply this as well.¹⁰

Further information on the nature of the mechanisms leading to products in this general mass region can be obtained from comparisons with models^{13, 26} or measurements^{16, 27} on the fission process. Mean momenta from the present experiment and other sources^{9, 12, 14, 28} are plotted in Fig. 5 as a function of product mass. Choice of symbols has been used to distinguish products with $Z_A - Z_{\text{eff}} > 0$ from those with $-2.0 < Z_A - Z_{\text{eff}} < 0$ and $Z_A - Z_{\text{eff}} < -2.0$. The curves shown in this figure are obtained from the solid-state detector measurements of Rensberg *et al.*^{16, 27} at 2.9 GeV.

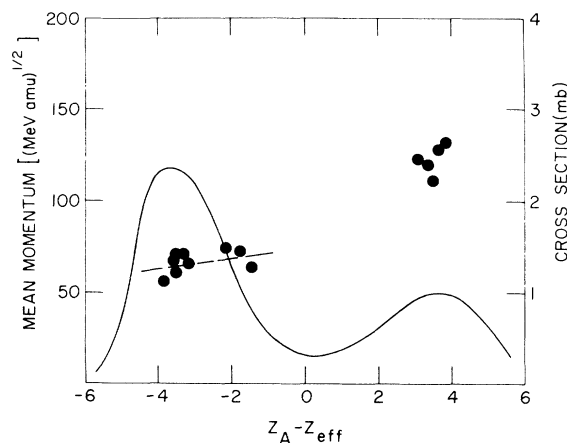


FIG. 4. Comparison between mean momenta and the charge-dispersion curve for rare-earth nuclides produced by the interaction of 28-GeV protons with uranium. Points indicate momenta of products having $139 \leq A \leq 156$. The solid curve is the charge dispersion reported for $A = 147$ (Ref. 10).

By selecting coincidence events in two detectors and from measurements of time of flight and energy, these authors obtained momentum spectra as a function of fragment mass for bonafide fission events. The upper curve (long dashed) shows the dependence of $\langle P \rangle$ on product mass observed for collinear fragments from a uranium target.¹⁶ The collinear geometry preferentially selects low deposition energy events and emphasizes asymmetric-mode fissions. As the correlation angle was changed away from 180° , the mean momentum for any mass fragment decreased. The solid curve in Fig. 5 gives the results for a group of fragments with correlation angles differing by 20° from collinearity.¹⁶ The lower-most curve (short dashed) in Fig. 5 is that observed for the fission of bismuth²⁷ by 2.9-GeV protons. There is essentially no variation of mean momenta with correlation angle for bismuth targets. The bismuth curve terminates at mass 145 in the figure indicating the yield of fragments had dropped to well below 0.1 mb/amu at that mass. Mean momenta for the neutron-rich group of products as determined radiochemically are seen to fall in the region of fission-fragment momenta observed by the solid-state detector study of uranium. We conclude that these represent the same sort of fission processes which

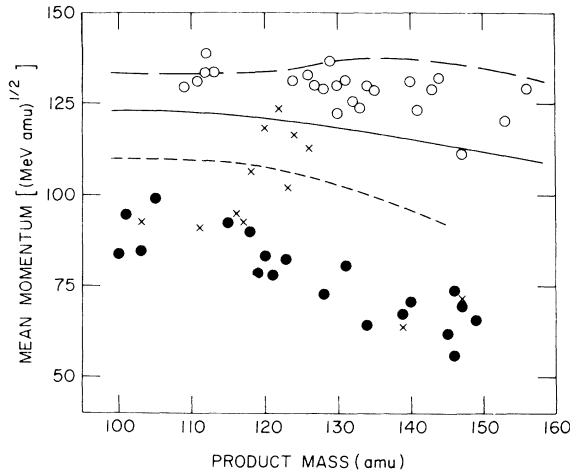


FIG. 5. Dependence of mean momenta on product mass for nuclides formed by the interaction of 10- to 28-GeV protons with uranium. Results from Refs. 9, 12, 14, 28, and the present work are combined. Symbols group products according to their distance from β stability: O, products having $Z_A - Z_{\text{eff}} > 0$; x, products with $-2 < Z_A - Z_{\text{eff}} < 0$; •, products with $Z_A - Z_{\text{eff}} < -2$. The lines present the results of semiconductor studies of fission induced by 2.9-GeV protons (Refs. 16, 27): The long-dashed line shows dependence of momentum on mass for collinear fragments in uranium fission; the solid line shows dependence for typical noncollinear fragments from uranium; the short-dashed line shows the dependence for the fission of bismuth.

were going on at 2.9 GeV. The slightly neutron-deficient products have lower mean momenta, some of which could be consistent with fission of lower-mass species. However, the highly neutron-deficient products ($Z_A - Z_{\text{eff}} < -2.0$) have momenta which fall well below those seen in the fission of bismuth. While it might be argued that still-lower-mass-fissioning species could be involved at 28 GeV, this ignores the problem of yields. The fission of species below bismuth must have negligible yields in the rare earth region (e.g. the yield from bismuth has fallen well below 0.1 mb/amu as noted above). The large yields of neutron-deficient products in the rare-earth region at 28 GeV^{10, 17} must arise for the most part from a process substantially different from binary fission. However, there may be small residual contributions from fission of excited species near uranium by the type of process which gives low yields of these products at 0.5 GeV and which continues to account for the neutron-rich products at 28 GeV.

We will use the term "spallationlike" to describe the dominant process leading to neutron-deficient rare-earth nuclides at 28 GeV. This may include spallation in a classical sense as well as contributions from processes involving light fragments. Crespo *et al.*²¹ have developed from general considerations of random addition of vectors an equation useful for the discussion of spallationlike reactions. The development below is somewhat modified from their approach.

When the velocity vector \vec{V} of a recoil nucleus can be considered as arising from addition of a number n of vectors \vec{V}_i each caused by the ejection of a particle mass m_i having velocity v_i , random walk theory and momentum conservation imply that

$$\langle V^2 \rangle = \sum_{i=1}^n \left[\frac{m_i v_i}{A_i} \right]^2. \quad (4)$$

In this equation A_i is the mass of the residual nucleus after emission of the i th particle. This sum can be expressed as n times the mean value, or

$$\langle V^2 \rangle = n \left\langle \left[\frac{m_i v_i}{A_i} \right]^2 \right\rangle. \quad (5)$$

We then make the approximation that A_i can be treated as a continuous variable and evaluate the mean in terms of the integrals as shown:

$$\langle V^2 \rangle = n \int_{A_0}^{A_T - m_1} \left[\frac{m_i v_i}{A_i} \right]^2 dA_i / \int_{A_0}^{A_T - m_1} dA_i. \quad (6)$$

In Eq. (6) the integrals are not to be evaluated over the whole range A_0 to A_T but only up to $A_T - m_1$, i.e., the target mass less the first emitted

particle. Since A_i is always positive and varies monotonically, the mean value theorem can be used to remove an average value of $\langle m_i^2 v_i^2 \rangle$ to obtain

$$\langle V^2 \rangle = \frac{n \langle m_i^2 v_i^2 \rangle}{A_0 (A_T - m_1)}, \quad (7)$$

where A_0 is the mass of the observed product. An estimate for n , the number of emitted particles, is the quotient of the mass difference and the mean mass of the emitted particles, $(A_T - A_0) / \langle m_i \rangle$. Substitution into Eq. (7) gives

$$\langle V^2 \rangle = \frac{\langle m_i^2 v_i^2 \rangle (A_T - A_0)}{\langle m_i \rangle A_0 (A_T - m_1)}. \quad (8)$$

It is convenient to consider kinetic energies rather than velocities in which case Eq. (8) transforms to

$$\langle T_0 \rangle = \langle t_i \rangle \frac{(A_T - A_0)}{(A_T - m_1)}. \quad (9)$$

Here it has been assumed that the mean kinetic energy of the emitted particles $\langle t_i \rangle$ is approximately equal to $\frac{1}{2} \langle m_i^2 v_i^2 \rangle / \langle m_i \rangle$. While many approximations have been made during the above derivation, it is expected that Eq. (9) will be useful in semiquantitative discussions of values of $\langle T_0 \rangle$ obtained from thick-target-thick-catcher recoil experiments. For spallation $\langle m_1 \rangle$ is small compared to A_T , and we can make the approximation that $A_T - m_1 \approx A_T$ in Eq. (9) to obtain the mean kinetic energy of the emitted particles from $\langle T_0 \rangle$ without a detailed knowledge of the number or type of particles involved. Values of $\langle t_i \rangle$ obtained from

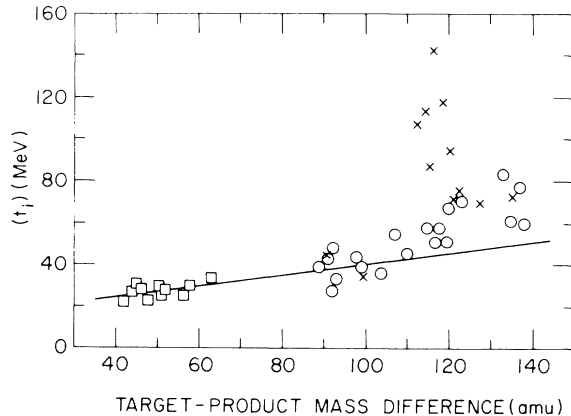


FIG. 6. Dependence of mean kinetic energy of emitted particles (as defined in text) on mass difference between target and product. Symbols denote different targets and product groups as follows: \square , rare-earth nuclides from gold (present work); \circ , highly neutron-deficient products ($Z_A - Z_{\text{eff}} < -2$) from uranium (Refs. 9, 12, 14, 28, and the present work); \times , products from uranium with $-2 < Z_A - Z_{\text{eff}} < 0$ (Refs. 9, 12, 14, 28, and the present work).

the mean kinetic energies given in Table IV for rare-earth nuclides produced by the interaction of 28-GeV protons with gold are plotted as a function of the target-product mass difference in Fig. 6. It might be expected that higher energies of excitation would be required to induce longer and longer evaporation cascades; hence, we would expect $\langle t_i \rangle$ to rise with increasing $A_T - A_0$. The gold data, shown as squares in Fig. 6 for $A_T - A_0$ values from 42 to 63, tend to show some increase as expected.

When values of $\langle t_i \rangle$ for highly neutron-deficient products from uranium are included in the figure, we see that the trend of the gold points runs through the neutron-deficient rare-earth points from uranium (at $A_T - A_0$ values of 89 to 104). The line shown is a least squares drawn through the gold points and those rare-earth points for which $Z_A - Z_{\text{eff}} < -2.0$. This line is within errors identical to that obtained from the gold points alone. We conclude that processes leading to neutron-deficient rare earths from uranium targets are smooth extrapolations of the processes operative in gold targets. The magnitude of the values of $\langle t_i \rangle$ can give information on the nature of the process. If only nucleons were involved, energies of 20 to 40 MeV would imply very high nuclear temperatures. On the other hand, experimental spectra²⁹ of complex particles ($Z \geq 2$) have means in this range, and it appears that such aggregates are in large part involved in what we have called the spallationlike process. It should be noted in Fig. 6 that some products with $A_T - A_0$ from ≈ 110 to ≈ 120 and with $-2 < Z_A - Z_{\text{eff}} < 0$ have $\langle t_i \rangle$ values which are quite large. This reflects the rise in momenta of these products as was seen in Fig. 3. That the values are so large is in part due to our approximation that $\langle m_1 \rangle \ll A_T$ in calculating $\langle t_i \rangle$ from $\langle T_0 \rangle$. For a symmetric fission process the error is a factor of 2 and we interpret the apparent $\langle t_i \rangle$ values of 100 to 140 MeV in Fig. 6 as indicating major contributions from fission to these slightly neutron-deficient products.

To this point our discussion has focused on momentum or kinetic energy imparted by the second step of the assumed two-step reaction mechanism. Information on the first step of the reaction is contained in the values of v_{\parallel} given in Tables III and IV. It is common practice to discuss not v_{\parallel} but a derived quantity, E^* , the cascade deposition energy. Porile³⁰ has pointed out that Monte Carlo calculations^{31,32} of intranuclear cascades show (on the average) a linear increase of E^* with v_{\parallel} . Values of E^* were calculated from v_{\parallel} values using the relationship

$$E^*/E_{\text{CN}} = 0.732 v_{\parallel} / v_{\text{CN}} \quad (10)$$

derived by Crespo *et al.*^{21,33} from 1.83-GeV proton induced cascades in Bi and U. In Eq. (10), E_{CN} and v_{CN} are the excitation energy and velocity of the hypothetical compound nucleus.

Values of E^* for rare-earth products from the interaction of 28-GeV protons with uranium are compared with values obtained by Hogan and Sugarman²⁵ at 0.44 GeV in Fig. 7. Points shown for the 0.44-GeV results differ somewhat from the published values as a consequence of our use of $N=1.34$ in Eq. (1) and the revised range-energy relationship. At the lower energy there is a nearly linear dependence of E^* on $Z_A - Z_{eff}$, with the neutron-rich species being formed in low-deposition energy processes and the deficient products at higher excitation energies. Results from the present experiment depend less strongly on $Z_A - Z_{eff}$ with the neutron-rich products having higher E^* values and the neutron-deficient ones having lower values of E^* than the corresponding products at 0.44 GeV. The weighted mean E^* of the neutron-rich products at 28 GeV is 118 MeV, for the deficient ones it is 145 MeV. Generally, higher E^* values are observed for products from gold at 28 GeV averaging 199 MeV.

We have noted in Fig. 6 that the mean kinetic energy of emitted particles in the spallationlike process increases as the product moves further from the target in mass. This is consistent with the general notion that longer evaporation cascades involve more excitation energy and higher nuclear temperatures than shorter ones. Plotted in Fig. 8 are E^* values for products from the interaction

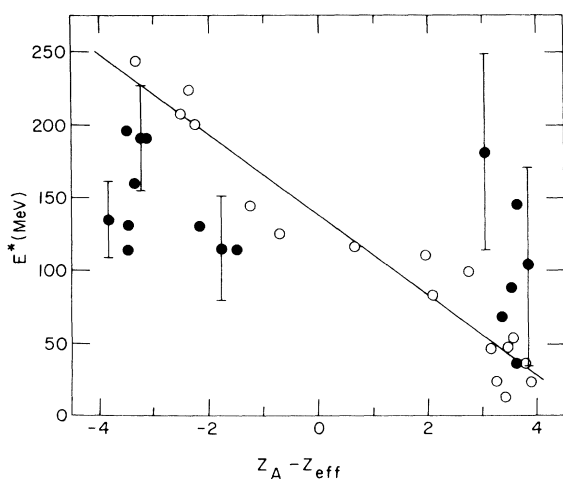


FIG. 7. Dependence of mean cascade deposition energy, E^* , on the distance of the product from β stability. Closed circles are from the present study of uranium at 28 GeV. Open circles show the results of Hogan and Sugarman (Ref. 25) obtained at 0.44 GeV. The line shows the trend of the low-energy results.

of 28-GeV protons with gold as measured in the present work and values for neutron-deficient products from uranium targets reported by several groups.^{9,14,28} We have not shown the anomalously high, 629-MeV value for ^{115}Sb (at $A_T - A_0 = 23$) reported by Hagebø and Ravn,¹⁴ nor are the results of Brandt¹² on iodine included. The latter indicate F/B ratios near unity for neutron-deficient products and it has been concluded that they do not give meaningful measures of forward momentum transfer. The dashed line in Fig. 8 shows the trend of the data. E^* does not increase with increasing $A_T - A_0$ but shows slightly the reverse effect. Furthermore, all the E^* values are much lower than would be expected for evaporation processes, e.g. calculations by Porile³⁴ have indicated E^* values of 500–600 MeV are necessary for ^{149}Tb production from Au and the results of Beg and Porile⁹ suggest $E^* \approx 900$ MeV for mass 131 production from U. In addition, as has been noted above, the procedure used in obtaining $v_{||}$ from the experimental data tends to yield values substantially larger than the true ones.

From the general independence of E^* on A as seen in Fig. 8 one can draw several possible conclusions. In the first place, a relationship between E^* and $v_{||}$ such as Eq. (10) may not be valid at very high energies. The general linear dependence of E^* on $v_{||}$ was inferred³⁰ from early Monte Carlo calculations extending up to an energy of 1.8 GeV. It is now confirmed by more detailed calculations³⁵ for energies up to 0.4 GeV. It is then still an open question whether a measurement of $v_{||}$ is an appropriate thermometer for measuring nuclear excitations at very high bombarding energies.

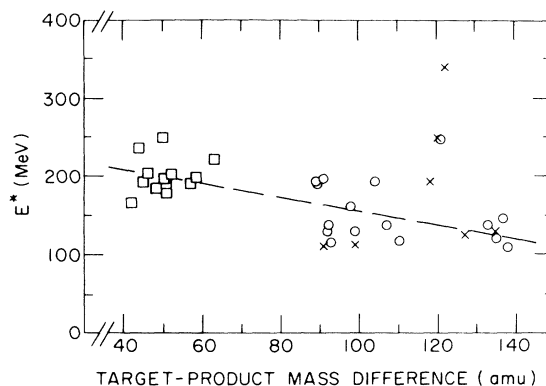


FIG. 8. Dependence of mean cascade deposition energy, E^* , on mass difference between target and product. \square , rare-earth nuclides produced from gold (present work); \circ , neutron-deficient products from uranium (Refs. 9, 14, 28, and the present work); \times , products from uranium with $-2 < Z_A - Z_{eff} < 0$ (Refs. 9, 14, 28, and the present work).

The other interpretation, a rather attractive one, is that the anomalously low v_{\parallel} values for neutron-deficient products reflect a breakdown of the two-step process. In this case preferential ejection of light fragments in the forward direction reduces the momentum of the precursors of the observed neutron-deficient products. Such preferential emission of light fragments is known for several target systems.^{29,36} Beg and Porile⁹ were able to quantitatively account for some of the recoil properties of ^{83}Sr and ^{131}Ba from U at 11.5 GeV in terms of a hybrid model in which a nucleonic cascade plus the experimental angular and energy distribution of ^{24}Na ejected from bismuth³⁶ was used to simulate an effective first stage of the reaction, combined with an evaporation second stage. While proof of the connection between light fragments and neutron-deficient products in the mass region we are considering must await the outcome of coincidence measurements,³⁷ such a connection does appear probable. In any event, it is clear that extrapolation to very high energies of Monte Carlo calculations in which only nucleon ejection is considered is not valid.

CONCLUSIONS

Recoil properties of rare-earth nuclides produced from uranium by 28-GeV protons follow the same general pattern seen for products of lower mass. Mean ranges of neutron-deficient isotopes are markedly reduced from those of the neutron-rich species. However, the difference between neutron-deficient and neutron-rich products is more pronounced in the rare-earth region, indicating a more clearcut distinction in reaction mechanisms. This supports a similar conclusion drawn from charge-dispersion measurements.

Mean momenta of neutron-rich species are in good agreement with momenta of the fission products as observed in the interaction of 2.9-GeV protons with uranium; hence conventional binary fis-

sion appears to be responsible for their formation even up to 28 GeV. The much lower momenta of neutron-deficient products cannot be explained in terms of the uranium or even the bismuth fission measurements at lower energies. Yield considerations rule out the fission of still lighter mass species as a mechanism.

Comparison of the properties of the neutron-deficient products from uranium with those of products from gold indicates a generally similar reaction mechanism characterized by low mean momenta (as measured by $\langle V \rangle$) and abnormally low mean forward momentum transfer (as measured by $\langle v_{\parallel} \rangle$). This latter point indicates a process distinctly different from spallation in the classical sense. The apparent values of E^* inferred from $\langle v_{\parallel} \rangle$ are too low for an evaporative second stage following an initial nucleonic cascade step. While fragment ejection in this first step is an attractive explanation for these observations it cannot be proven by experiments such as the present one. There is increasing evidence that fragments are, at least in part, ejected on the same time scale as the prompt nucleonic cascade. It is clear, then, that they cannot be ignored in any calculations which predict detailed recoil properties at GeV energies.

ACKNOWLEDGMENTS

The authors are indebted to many colleagues for helpful discussions and suggestions during the present work. One of us (K.B.) wishes to acknowledge the hospitality of the Chemistry Department of Brookhaven National Laboratory during the time he spent there. We would like to express our appreciation to the many persons who contributed to the completion of this work: Dr. J. Hudis for assistance during the irradiations, Miss E. M. Franz for help during the chemical separations, Mrs. E. Rowland for some of the sample assays, and Dr. R. W. Stoenner and Miss. E. Norton for the chemical yield determinations.

*Research performed under the auspices of the U. S. Atomic Energy Commission.

†Present address: Lehrstuhl für Kernchemie, Eduard-Zintl-Institut, Technische Hochschule, 61 Darmstadt, Germany.

¹G. Friedlander, L. Friedman, G. Gordon, and L. Yaffe, *Phys. Rev.* **129**, 1809 (1963).

²J. M. Alexander, C. Baltzinger, and M. F. Gazdik, *Phys. Rev.* **129**, 1826 (1963).

³G. Friedlander, in *Proceedings of the Symposium on the Physics and Chemistry of Fission, Salzburg, 1965* (International Atomic Energy Agency, Vienna, Austria, 1965), Vol. 2, p. 265.

⁴G. Rudstam and G. Sørensen, *J. Inorg. Nucl. Chem.* **28**, 771 (1966).

⁵E. Hagebø, *J. Inorg. Nucl. Chem.* **29**, 2515 (1967).

⁶R. Klapisch, J. Chaumont, J. Jastrzebski, R. Bernas, G. N. Simonoff, and M. Lagarde, *Phys. Rev. Letters* **20**, 743 (1968).

⁷J. Chaumont, Ph.D. thesis, Université de Paris, 1970 (unpublished).

⁸J. Hudis, T. Kirsten, R. W. Stoenner, and O. A. Schaeffer, *Phys. Rev. C* **1**, 2019 (1970).

⁹K. Beg and N. T. Porile, *Phys. Rev. C* **3**, 1631 (1971).

¹⁰Y. Y. Chu, E. M. Franz, G. Friedlander, and P. J. Karol, *Phys. Rev. C* **4**, 2202 (1971).

¹¹Z_A - Z is the distance from the line of β stability along an isobaric chain.

¹²R. Brandt, in *Proceedings of the Symposium on the Physics and Chemistry of Fission, Salzburg, 1965* (International Atomic Energy Agency, Vienna, Austria, 1965), Vol. 2, p. 329; *Radiochim. Acta* **16**, 148 (1972).

¹³V. P. Crespo, J. B. Cumming, and A. M. Poskanzer, *Phys. Rev.* **174**, 1455 (1968).

¹⁴E. Hageböll and H. Ravn, *J. Inorg. Nucl. Chem.* **31**, 2649 (1969).

¹⁵K. Bächmann and J. B. Cumming, *Phys. Rev. C* **5**, 210 (1972).

¹⁶L. P. Remsberg, F. Plasil, J. B. Cumming, and M. L. Perlman, *Phys. Rev.* **187**, 1597 (1969).

¹⁷K. Bächmann, *J. Inorg. Nucl. Chem.* **32**, 1 (1970).

¹⁸N. Sugarman, M. Campos, and K. Wielgoz, *Phys. Rev.* **101**, 388 (1956); N. T. Porile and N. Sugarman, *Phys. Rev.* **107**, 1410 (1957).

¹⁹J. B. Niday, *Phys. Rev.* **121**, 1471 (1961).

²⁰For a general review, see J. M. Alexander, in *Nuclear Chemistry*, edited by L. Yaffe (Academic, New York, 1968), Vol. I, p. 273.

²¹V. P. Crespo, J. B. Cumming, and J. M. Alexander, *Phys. Rev. C* **2**, 1777 (1970).

²²N. Sugarman, H. Münzel, J. A. Panontin, K. Wielgoz, M. V. Ramaniiah, G. Lange, and E. Lopez-Menchero, *Phys. Rev.* **143**, 952 (1966).

²³J. B. Cumming, unpublished.

²⁴L. C. Northcliffe and R. F. Schilling, *Nucl. Data* **A7**,

233 (1970).

²⁵J. J. Hogan and N. Sugarman, *Phys. Rev.* **182**, 1210 (1969).

²⁶J. R. Nix and W. J. Swiatecki, *Nucl. Phys.* **71**, 1 (1965).

²⁷L. P. Remsberg, F. Plasil, J. B. Cumming, and M. L. Perlman, *Phys. Rev. C* **1**, 265 (1970).

²⁸J. A. Panontin and N. T. Porile, *J. Inorg. Nucl. Chem.* **32**, 1775 (1970).

²⁹A. M. Poskanzer, G. W. Butler, and E. K. Hyde, *Phys. Rev. C* **3**, 1 (1971).

³⁰N. T. Porile, *Phys. Rev.* **120**, 572 (1960).

³¹N. Metropolis, R. Bevins, M. Storm, A. Turkevich, J. M. Miller, and G. Friedlander, *Phys. Rev.* **110**, 185 (1958).

³²N. Metropolis, R. Bevins, M. Storm, J. M. Miller, G. Friedlander, and A. Turkevich, *Phys. Rev.* **110**, 204 (1958).

³³In Ref. 21 the constant term in Eq. (10) appears on the opposite side of the equation due to an error.

³⁴N. T. Porile, private communication as quoted in Ref. 21.

³⁵K. Chen, Z. Fraenkel, G. Friedlander, J. R. Grover, J. M. Miller, and Y. Shimamoto, *Phys. Rev.* **166**, 949 (1968).

³⁶J. B. Cumming, R. J. Cross, Jr., J. Hudis, and A. M. Poskanzer, *Phys. Rev.* **134**, B167 (1964).

³⁷D. Perry and L. P. Remsberg, unpublished.

Positron Branching in the Decay of ¹⁴³Sm, ¹⁴¹Nd, and ¹⁴⁰Pr

J. L. Evans, J. R. Cooper, D. M. Moore, and W. L. Alford

Physics Department, Auburn University, Auburn, Alabama 36830

(Received 22 May 1972)

The nuclides ¹⁴³Sm, ¹⁴¹Nd, and ¹⁴⁰Pr were prepared by the (*n*, 2*n*) reaction using energetic neutrons produced by deuteron bombardment of tritium and lithium targets. A comparison of *K* x rays and annihilation radiation from each nuclide was made by means of a thin-window NaI detector. Using theoretical ratios of *K* electron capture to total electron capture, percentages of positron emission for ¹⁴³Sm, ¹⁴¹Nd, and ¹⁴⁰Pr were found to be 40.0 ± 2.0, 2.72 ± 0.20, and 48.7 ± 2.2, respectively.

INTRODUCTION

For a number of (*n*, 2*n*) reactions, neutron deficient nuclides are produced for which positron emission is a possible mode of decay. Since it is quite common practice to determine cross sections for such reactions by measuring the induced positron activities, a knowledge of the ratio of electron capture to positron emission in the decay of the product nucleus is essential. Our interest in certain rare earth isotopes has led us to measure the percentages of positron emission in the decay of

¹⁴³Sm, ¹⁴¹Nd, and ¹⁴⁰Pr. The purpose of this paper is to describe briefly these measurements.

EXPERIMENTAL PROCEDURE AND RESULTS

Deuterons from the Auburn University dynamitron accelerator were used to produce energetic neutrons by the T(*d*, *n*)⁴He and ⁷Li(*d*, *n*)⁸Be reactions. Samples subjected to neutron irradiation consisted of 0.0971 g of 99.9% pure powdered Pr₆O₁₁, 0.233 g of Nd₂O₃ enriched to greater than